ELSEVIER

Journal of Alloys and Compounds 356–357 (2003) 200–203

Journal of ALLOYS AND COMPOUNDS

www.elsevier.com/locate/jallcom

Structural, magnetic and hyperfine properties of $Zr(Cr_{1-x}Fe_x)_2$ hydrides

J.A.H. Coaquira[a], H.R. Rechenberg[a,*], J. Mestnik-Filho[b], A.W. Carbonari[b]

[a]Instituto de Física, Universidade de São Paulo, C.P. 66318, 05315-970 São Paulo, Brazil
[b]Instituto de Pesquisas Energéticas e Nucleares, C.P. 11049, 05422-970 São Paulo, Brazil

Received 1 June 2002; accepted 25 October 2002

Abstract

Laves-phase compounds with the hexagonal C14-type structure $Zr(Cr_{1-x}Fe_x)_2$ ($x=0.3$–0.7) were charged to maximum H capacity, which ranged from 3.6 to 2.5 H/f.u. for increasing x. The biggest cell volume expansion was 22%. Magnetic properties were investigated with magnetometry and Mössbauer spectroscopy. The hydrides exhibited spin-glass behavior, similar to their parent compounds, but with larger Fe moments and lower freezing temperatures. Electric hyperfine interactions were measured in the 78–350 K temperature range at the Fe sites and at the Zr site, using ^{57}Fe MS and ^{181}Ta TDPAC, respectively. Activation energies for H jump diffusion were determined by these two complementary techniques, yielding 72(4) and 246(30) meV respectively.

Keywords: Zr-based Laves phase; Magnetic properties; Mössbauer spectroscopy; Perturbed angular correlations; Hydrogen diffusion

1. Introduction

$Zr(Cr_{1-x}Fe_x)_2$ Laves phase compounds are known for their hydrogen storage capacity, which is 3.8 H/mol for $ZrCr_2$ and remains appreciable up to $x\approx0.7$ [1]. While the end compounds crystallize in the C15 cubic structure, a change to the C14 hexagonal structure occurs in the $x\approx$ 0.3–0.8 range [2]. Structural and magnetic studies on the hexagonal $Zr(Cr_{1-x}Fe_x)_2$ alloys have been reported recently [3,4]; the changes induced on these properties by H absorption are discussed in this work. In addition, the temperature dependence of hyperfine parameters in $Zr(Cr_{0.5}Fe_{0.5})_2$ hydride has been measured by means of two complementary techniques, the ^{57}Fe Mössbauer resonance at the Fe sites and the time-differential perturbed angular correlation (TDPAC) of γ-rays from ^{181}Ta formed after β decay of ^{181}Hf located at the Zr site. These data provided information on H atomic jump diffusion.

2. Experimental

As-cast samples with $x=0.3$–0.7, prepared by arc melting under pure argon, were hydrogen charged in a Sievert-type facility at ~1 atm. pressure by slowly cooling from 800 °C to room temperature. The absorbed H amount was determined from the sample's mass increase. X-ray powder diagrams were obtained with CuKα radiation and analyzed by the Rietveld method. VSM and SQUID magnetometers were used for magnetic measurements. Mössbauer spectra were obtained in the constant-acceleration mode using a Rh(^{57}Co) source. One additional sample, of composition $Zr(Cr_{0.5}Fe_{0.5})_2H_{2.7}$, was prepared incorporating radioactive ^{181}Hf onto the Zr site at the melting stage. TDPAC measurements were performed with a four BaF_2 detectors set-up, with a time resolution of 0.8 ns.

3. Results and discussion

XRD analysis showed that the hexagonal C14 structure was retained for all samples after hydrogen charging. The absorbed H amounts and resulting volume expansions are given in Table 1. The specific volume increase was $dV/dn=3.1\times10^{-3}$ nm^3 per H atom. The volume expansion was anisotropic, as indicated by the mean c/a ratio change from 1.640 to 1.631 on hydrogenation. Hydride formation was not complete for the $x=0.7$ alloy, as indicated by the presence of a low-hydrogen solid solution with $\Delta V/V\approx1\%$

---

*Corresponding author. Tel.: +55-11-3091-6877; fax: +55-11-3091-6984.

E-mail address: hercilio@macbeth.if.usp.br (H.R. Rechenberg).

0925-8388/02/$ – see front matter
doi:10.1016/S0925-8388(02)01235-5

Table 1
Composition x, number of H atoms per formula n, magnetic moment per Fe atom $\langle \mu_{Fe} \rangle$, spin freezing temperature from ac susceptibility T_f for $Zr(Cr_{1-x}Fe_x)_2H_n$; corresponding magnetic quantities for the parent alloys [4] are given in the last two columns

x	n	$\Delta V/V$ (%)	$Zr(Cr_{1-x}Fe_x)_2H_n$ $\langle \mu_{Fe} \rangle$ (μ_B)	$Zr(Cr_{1-x}Fe_x)_2H_n$ T_f (K)	$Zr(Cr_{1-x}Fe_x)_2$ $\langle \mu_{Fe} \rangle$ (μ_B)	$Zr(Cr_{1-x}Fe_x)_2$ T_f (K)
0.3	3.6	20.9	0.43	3.9	0.17	3.3
0.4	3.7	22.4	0.68	8.3	0.30	10.5
0.5	3.3	19.3	0.84	15.6	0.34	20.5
0.6	3.0	17.8	1.02	27.4	0.47	32.1
0.7	2.5	16.6	1.22	39.5	0.67	45.6

(α phase) in addition to the full hydride (β phase), amounting to 30% of the sample. Detailed X-ray data are found in Ref. [3].

Magnetization curves measured at $T = 4.2$ K are shown in Fig. 1. Magnetic saturation was not reached in the available field range for any sample. Saturation moments were estimated by linear extrapolation to $1/H \rightarrow 0$; such data are given in Table 1 in Bohr magnetons per Fe atom (assuming Cr atoms to carry no moment). An Arrott-plot analysis of the $M(H)$ data revealed that none of the hydrides exhibit spontaneous magnetic ordering. Instead, all samples were found to undergo spin-glass freezing at a temperature T_f indicated by a sharp peak in the susceptibility vs. T curve. Spin freezing was further confirmed through Mössbauer spectroscopy (MS) at low temperatures. The spectra at $T = 4.2$ K were magnetically split sextets with broad overlapping lines. Good fits were achieved with a hyperfine field distribution $P(B_{hf})$, whence a mean $\langle B_{hf} \rangle$ was obtained. $\langle B_{hf} \rangle$ decreased at increasing temperatures, vanishing at a temperature ~1.25 T_f (i.e. the spin freezing temperature probed on the MS time scale $\sim 10^{-8}$ s [5]).

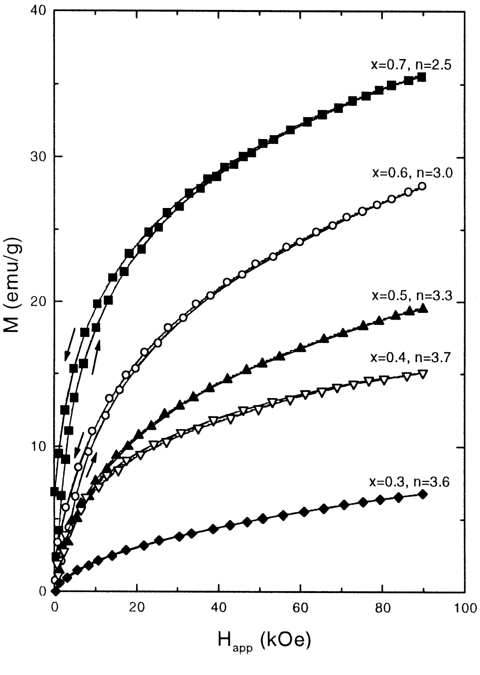

Fig. 1. Magnetization curves of indicated samples, measured at $T = 4.2$ K.

The parent $Zr(Cr_{1-x}Fe_x)_2$ alloys ($x = 0.3$–0.7) also exhibit spin-glass behavior, in a qualitatively similar way to their hydrides [4]. Data for both groups of materials are given in Table 1. Comparing each alloy with the corresponding hydride, one sees that H absorption enhances the Fe moment, but its effect on T_f is a moderate decrease. Both effects are illustrated by the temperature dependence of $\langle B_{hf} \rangle$ for $Zr(Cr_{0.4}Fe_{0.6})_2$ and $Zr(Cr_{0.4}Fe_{0.6})_2H_3$, shown in Fig. 2. These apparently contradictory trends can be rationalized by assuming the cell volume expansion to be the main effect of hydrogen inclusion: while the 3d band becomes narrower, resulting in a larger Fe moment, the average Fe–Fe distances increase, weakening the exchange interactions.

Mössbauer spectra of a $Zr(Cr_{0.5}Fe_{0.5})_2H_{3.3}$ sample were measured in the 78–350 K temperature range. The spectra have been fitted with two quadrupolar doublets with a 3:1 area ratio, corresponding to the 6h and 2a sites occupied by Fe in this structure. A pronounced QS temperature dependence was found at the 6h Fe site, while QS at the 2a site was nearly constant. Taking into account the experimental H occupancy among all possible interstitial sites [6], it can be shown [3] that 6h sites are more likely than 2a to have an H atom as a close neighbor, therefore the observed effect must be related to H motion. We assume the observed QS to be a time average over two configurations: QS_{eq} with H in an equilibrium position, and a smaller QS_{tr} when H is jumping between two such sites. Using a simple model [7] one obtains

$$QS(T) = \frac{QS_{eq}\tau_{res} + QS_{tr}\tau_{jump}}{\tau_{res} + \tau_{jump}} \tag{1}$$

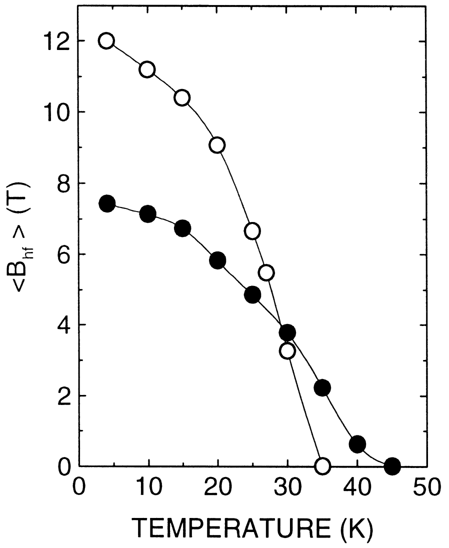

Fig. 2. Mean hyperfine field temperature dependence of $Zr(Cr_{0.4}Fe_{0.6})_2$ (full symbols) and $Zr(Cr_{0.4}Fe_{0.6})_2H_3$ (open symbols).

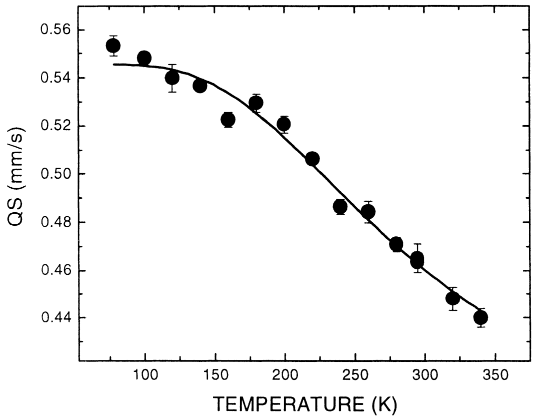

Fig. 3. $Zr(Cr_{0.5}Fe_{0.5})_2H_{3.3}$ quadrupole splitting at 6*h* Fe site vs. temperature. Curve: fit to Eq. (1).

with $\tau_{res} = \tau_0 \exp(E/kT)$ ($\tau_0 \approx 10^{-13}$ s) and a constant $\tau_{jump} \approx 10^{-12}$ s. From a fit to the data (Fig. 3) an activation energy $E = 72(4)$ meV was obtained. Other fitting parameters were $QS_{eq} = 0.55$ mm/s and $QS_{tr} = 0.32$ mm/s.

The motions of hydrogen atoms within $ZrCrFeH_{2.7}$ were also observed by means of the time differential perturbed angular correlation (TDPAC) technique. The TDPAC of gamma rays enables one to determine the hyperfine fields acting on nuclei of suitable probe atoms, as ^{181}Ta substituting Zr in the present case. The measured quantity is the time modulation of the angular anisotropy of a γ–γ cascade of the probe nucleus, given by $A_{kk}G_{kk}(t)$ with A_{kk} the unperturbed anisotropy and $G_{kk}(t)$ accounting for the perturbation caused by the interaction of the probe nucleus with external fields such as the electric field gradient (EFG) due to the electronic cloud and external charges [8]. Usually only the $k = 2$ term is retained. When a probe atom is surrounded by moving hydrogen atoms, a fluctuating EFG is observed as a relaxation of the perturbation function that can be approximated by $G_{kk}(t) = \Gamma_{kk}(t) \cdot \exp(-\lambda_k t)$ [9]. $\Gamma_{kk}(t)$ is dependent on the relative time scale of hydrogen motions as compared to the TDPAC time window: in the slow fluctuation regime, $\Gamma_{kk}(t)$ is the same as the static perturbation, i.e.

$$\Gamma_{kk}(t) = s_{k0} + \sum_{k=1}^{N} s_{kn} \cos(\omega_n t) \exp\left[-1/2(\delta\omega_n t)^2\right] \qquad (2)$$

where ω_n are the transition frequencies between the nuclear hyperfine levels, and the exponential factor accounts for a gaussian EFG distribution with relative width $\delta\omega_n$. In the fast fluctuating regime $\Gamma_{kk}(t)$ is the perturbation function that corresponds to a time average of the fluctuating EFG (see [9] for further details). Within this regime $\lambda_k \propto w^{-1}$ where w is the time rate of EFG fluctuation. If the latter can be expressed by an Arrhenius law, $w = w_0 \cdot \exp(-E_a/kT)$, an activation energy for hydrogen jumps can be deduced from the temperature dependence of $\ln \lambda_k$.

Fig. 4 displays the measured perturbed angular correlation coefficient $-A_{22}G_{22}(t)$ ($A_{22} = -0.282$ for ^{181}Ta probe) for $ZrCrFeH_{2.7}$ at temperatures of 120, 175 and 340 K, corresponding, respectively, to the static, slow and fast fluctuation regimes.

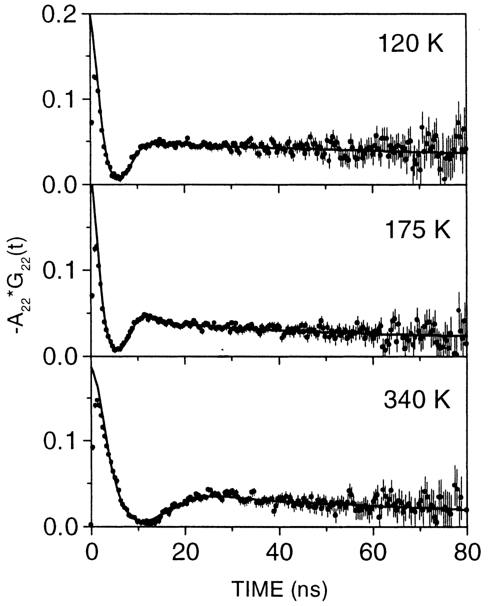

Fig. 4. TDPAC spectra of $ZrCrFeH_{2.7}$ at the indicated temperatures, corresponding to different regimes of hydrogen motion (see text).

Skripov et al. [10] observed two distinct hydrogen hopping rates in the $ZrCr_2$ hydride and ascribed them to two different motions of hydrogen atoms with different time scales: one within hexagons that share the same two Zr atoms, the other between hexagons that do not. The first motion restricts the hydrogen atoms to a confined space whereas the second one enables long range diffusion. This model is valid for both the C14 and C15 crystalline structures.

The dynamic effects observed in the present study are more probably related to the hydrogen atoms moving within one hexagon, i.e., the first kind of motion referred to above. This is because at higher temperatures, say $T > 300$ K, the fast fluctuating regime is observed in which many hydrogen jumps occur within the TDPAC time window. On the contrary, if the motion is such that a hop is performed to a neighboring hexagon and the hydrogen atom leaves the current probe atom, it is expected that the hyperfine parameters would present a second component similar to a static EFG.

Fig. 5 presents a plot of $\ln \lambda_2$ as a function of the inverse of the temperature where the two distinct dynamic regimes, slow and fast fluctuations, can be observed. From the slope of the left-hand straight line, corresponding to the fast fluctuations, an activation energy $E_a = 246(30)$ meV results for the localized hydrogen motions around a Ta probe substituting a Zr atom. Due to the fact that the probe atom is not a host Zr atom, a slightly different activation energy for motions around Zr atoms can be expected.

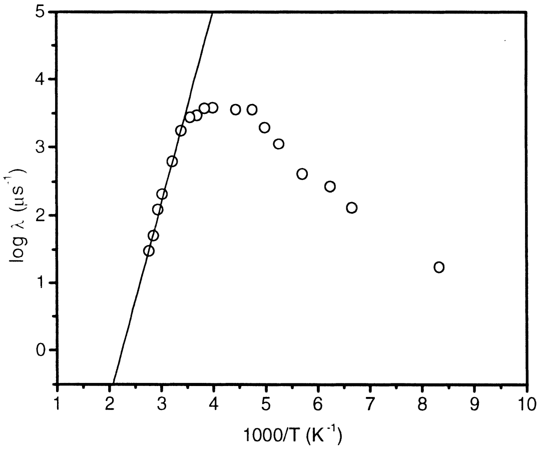

Fig. 5. Logarithm of the relaxation parameter λ_2 as a function of the inverse of temperature. Straight line is a fit to Arrhenius' law.

However, the activation energy deduced here agrees quite well with a nuclear magnetic resonance measurement performed on $ZrCr_2$ [11].

The large discrepancy between the activation energies obtained from MS and TDPAC data is noteworthy. As already noted above, two kinds of H motion, with different characteristic times, have been identified in Laves-phase hydrides [10]. Our MS and TDPAC measurements probed the immediate environment of nuclei situated at distinct lattice sites, each of which could possibly be more sensitive to a specific type of H atomic jump, depending on the local symmetry. Theoretical EFG calculations for different interstitial hydrogen configurations would be helpful to clarify this point.

Acknowledgements

This work was financially supported by CNPq and FAPESP.

References

[1] D. Shaltiel, I. Jacob, D. Davidov, J. Less-Common Met. 53 (1977) 117.
[2] K. Kanematsu, J. Phys. Soc. Jpn. 29 (1970) 864.
[3] J.A.H. Coaquira, H.R. Rechenberg, J. Mestnik Filho, J. Alloys Comp. 288 (1999) 42.
[4] J.A.H. Coaquira, H.R. Rechenberg, J. Phys.: Condens. Matter 13 (2001) 8415.
[5] J.A. Mydosh, Spin Glasses: An Experimental Introduction, Taylor and Francis, London, 1993.
[6] O. Canet, M. Latroche, F. Bourée-Vigneron, A. Percheron-Guégan, J. Alloys Comp. 210 (1994) 129.
[7] K. Negita, N. Nakamura, H. Chihara, Chem. Phys. Lett. 63 (1979) 187.
[8] E. Karlson, E. Mathias, K. Siegbahn (Eds.), Perturbed Angular Correlations, North-Holland, Amsterdam, 1964, Chapter 1.
[9] M. Forker, W. Herz, D. Simon, Nucl. Instrum. Methods Phys. Res. A 337 (1994) 534.
[10] A.V. Skripov, M. Pionke, O. Randl, R. Hempelmann, J. Phys.: Condes. Matter 11 (1999) 1489.
[11] R.D. Stoddard, J. Balbach, M.S. Conradi, A.V. Skripov, Phys. Rev. B 59 (1998) 3769.